PAPER

Check for updates

Access to ligand-stabilized PH-containing phosphenium complexes†

David Biskup, [ID] [a] Gregor Schnakenburg, [ID] [a] Arturo Espinosa Ferao [ID] *[b] and Rainer Streubel [ID] *[a]

While the chemistry of phosphenium compounds, including metal complexes thereof, is very well established, few derivatives having a P–H bond have been described, yet. This work describes rational access to donor-stabilised phosphenium metal complexes possessing a P–H bond using protonation reactions of stable phosphinidene complex adducts. While most Brønsted–Lowry acids yield formal 1,1-addition products at the phosphorus centre under the loss of the donor, super-strong acids having weakly coordinating anions enable access to donor-stabilised P–H phosphenium complex salts. The latter possess *N*-methylimidazole as a donor (to phosphorus) and the N–P interaction has been studied theoretically.

Introduction

The first cationic dicoordinate phosphorus compounds, namely, phosphamethinecyanines, were described by Dimroth and Hoffmann in 1964, being stabilised by π-donation of the electron-rich neighbouring atoms and charge delocalization.[1] Afterwards, a broad range of compounds containing phosphenium cations stabilised by π-donor-substituents were described, *e.g.* amino(aryl)phosphenium salts,[2] diamino phosphenium salts,[2] 1,3,2-diazaphospholidinium salts,[3] 1,3,2-diazaphosphinanium salts,[4] or 1*H*-1,2,3-diazaphospholium salts.[5] The latter, analogues of N-heterocyclic carbenes, were first prepared by Pudovik[6] and Denk,[7] and further intensely investigated by Gudat.[8] Niecke and Kröher reported a zwitterionic metallaphosphenium salt in 1976.[9] Recently, the synthesis of a kinetically stabilised donor-free phosphenium salt **I** was reported by Olaru, Mebs and Beckmann (Fig. 1).[10] Phosphenium salts are usually prepared *via* halide abstraction of halophosphanes.[11] A different access was described by Niecke *via* the protonation of a phosphaalkene[12] or an iminophosphane[13] and later by Grützmacher through methylation of a diphosphene derivative.[14] The chemistry of donor-to-nonmetal element adducts started with a report of Burford on cationic low-coordinate phosphorus species such as phosphadiazonium and phosphenium adducts.[15]

Similar to carbene metal complexes, PR$_2$ metal complexes can show an electrophilic or nucleophilic character dependent on the nature of the metal, its co-ligands and the PR$_2$ fragment itself.[16] Hence, the P-centre can behave as either a phosphenium or a phosphido ligand. The majority of phosphenium complexes are cationic but neutral complexes have also been described in literature.[16] However, cationic phosphido complexes are exceptional and were only obtained by using electron-rich metal centres without π-acidic co-ligands.[16]

Several pathways to phosphenium metal complexes were described including ligand substitution, salt metathesis, alkoxy abstraction, halide abstraction and elimination reactions.[16,17] Reactions of phosphenium complexes with neutral nucleophiles were only investigated sparsely, predominantly by Nakazawa and Gudat. In many cases, reactions were observed at the metal instead of the P centre and thus, to date, the class of donor-to-phosphenium complex adducts have been only rarely reported.[17–19] Very recently, Ragogna and Gilroy described the first N-donor-to-phosphenium complex adducts **II** where the N-donor centre was tethered as *P*-substituent (Fig. 1).[18] The first non-stabilised P–H functional
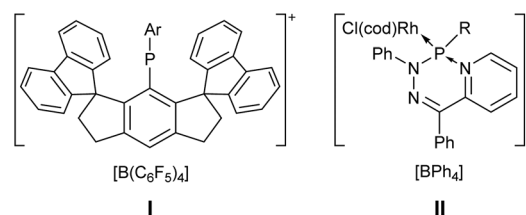
[a]Institut für Anorganische Chemie, Rheinische Friedrich-Wilhelms-Universität Bonn, Gerhard-Domagk-Str. 1, 53121 Bonn, Germany. E-mail: r.streubel@uni-bonn.de
[b]Departamento de Química Orgánica, Facultad de Química, Campus de Espinardo, Universidad de Murcia, 30100 Murcia, Spain. E-mail: artuesp@um.es
†Electronic supplementary information (ESI) available. CCDC 2302946–2302953. For ESI and crystallographic data in CIF or other electronic format see DOI: https://doi.org/10.1039/d3dt03869f

Fig. 1 The first stable donor-free phosphenium salt **I** and the first N-donor-to-phosphenium complex **II**.[10,18]

phosphenium complex was reported by Schrock and Churchill in 1982.[20] Afterwards, only a few further examples were described and sparsely investigated.[16,21] In 2007 Delpech reported on the protonation and alkylation of a terminal phosphinidene ruthenium complex to yield respective phosphenium complexes.[22] Reactions of a terminal phosphinidene complex with dihydrogen yielded only primary phosphane complexes or respective diphosphane complexes.[23] The first transition-metal-free N-heterocyclic carbene-to-phosphenium adduct bearing a P–H unit was reported by Bertrand, but this inversely polarised *P*–H phosphaalkene[24] should be better named as a zwitterion, *i.e.*, imidazolium phosphanide.

The question came up if neutral electrophilic, terminal phosphinidene complexes[25] bearing only π-acidic co-ligands might be used, somehow, to access *P*–H substituted phosphenium complexes. Such phosphinidene complexes were intensely studied *via* thermal chelotropic elimination or extrusion-type chemistry using 7-phosphanorbornadiene,[26] phosphirane,[27] 2*H*-azaphosphirene[28] or phosphepine complexes.[29] An alternative access to such species, usually generated at elevated temperatures, can be achieved *via* M/X phosphinidenoid complexes at low temperatures. So far, a broad scope of nucleo- and electrophilic chloride substitution reactions, ring expansion reactions, 1,2-addition to polar π-systems, oxidative single electron transfer reactions and the formal insertion reactions into OH- or NH-bonds were identified during the past years.[30] A first attempt to synthesise an imidazole-stabilised transient electrophilic terminal phosphinidene complex was undertaken by Mathey in 2006. He studied the reaction of a 7-phosphanorbornadiene complex with N-methylimidazole at elevated temperatures, but only cyclic polyphosphanes were obtained as final products when no trapping reagents were present; therefore, the adduct was only proposed as an intermediate.[31] Very recently, we reported on the synthesis and isolation of the first N-methylimidazole-to-phosphinidene complex adduct which could release an electrophilic, terminal phosphinidene complex under mild conditions. But we also observed a stunning thermal decomposition to yield white phosphorus as a final product when no trapping reagents were present.[32] Donor-to-phosphinidene complex adducts are expected to exhibit an increased negative charge at phosphorus compared to the genuine phosphinidene complexes showing a less pronounced electrophilic behaviour, *i.e.* reactions with stronger donors occurred while no reactivity towards alkenes could be observed at ambient temperature.[32,33] Therefore, an ambiguous reactivity of the donor-to-phosphinidene complex adducts is expected also enabling *P*-nucleophilic reactions.

Herein, we report on the reactivity of an N-methylimidazole-to-phosphinidene complex adduct towards a wide variety of Brønsted–Lowry acids intending to gain access to isolable donor-to-phosphenium complex adducts as potential precursors for genuine *P*–H substituted phosphenium complexes. The reaction pathway of the 1,1-addition of methanol has been computationally studied as a case in point. Furthermore, the varying donor-to-phosphorus interactions were inspected.

Results and discussion

Insertion reactions with water and alcohols

While (almost) no reactivity towards water has been observed for *P*-CPh$_3$ substituted Li/Cl phosphinidenoid group 6 metal complexes, surprisingly, the N-methylimidazole-to-phosphinidene complex adduct **1** exhibited high reactivity towards water. The formation of hydroxy(triphenylmethyl)phosphane complex **2** strongly bound to N-methylimidazole (N-MeIm) *via* O–H⋯N hydrogen bonding was observed (Scheme 1).

The ^{31}P NMR spectrum of **2**·*N*-MeIm in THF-d_8 displays a single resonance signal at 94.7 ppm ($^1J_{P,H}$ = 337 Hz, $^1J_{W,P}$ = 267 Hz), and the presence of one equivalent of N-methylimidazole was identified in the ^{1}H NMR spectrum. Additionally, the OH proton resonance is strongly deshielded showing a slightly broadened signal at 12.94 ppm, indicating a rather strong hydrogen bonding to the N^3 atom of the N-MeIm unit. The N-MeIm was not separable from complex **2** *via* evaporation *in vacuo* (<0.02 mbar) or *via* recrystallization. However, a clean separation was achieved *via* column chromatography at ambient temperature using an *n*-pentane/diethyl ether mixture as the eluent under argon atmosphere (Scheme 1).

The ^{31}P NMR signal of **2** appears slightly downfield-shifted compared to **2**·*N*-MeIm at 99.2 ppm ($^1J_{P,H}$ = 341 Hz, $^1J_{W,P}$ = 270 Hz). In the ^{1}H NMR spectrum of **2**, the resonance of the OH group shifted upfield by 4.55 ppm to 8.39 ppm, revealing the loss of the hydrogen bonding to N-MeIm. This tendency was even stronger if a weaker coordinating solvent such as dichloromethane-d_2 was used; here, the resonance appeared at 3.79 ppm ($^2J_{P,H}$ = 5 Hz). The other proton resonances changed only marginally when transitioning from **2**·*N*-MeIm to pure **2** or by changing the solvent. The solvent change has almost no effect on the ^{31}P resonance, as the signal shifted from 99.2 to 100.7 ppm. The molecular structure of complex **2** was confirmed by single-crystal X-ray diffraction analysis (Fig. 2).

The reaction of complex **1** with methanol and *tert*-butanol gave the OH insertion products **3a** (δ(^{31}P) = 127.2 ppm, $^1J_{P,H}$ = 343 Hz, $^3J_{P,H}$ = 13 Hz, $^1J_{W,P}$ = 274 Hz) and **3b** (δ(^{31}P) = 97.4 ppm, $^1J_{P,H}$ = 322 Hz, $^1J_{W,P}$ = 283 Hz) (Scheme 2). Previously, we reported on these products using a different approach.[34] In this study, the reaction progress decreased
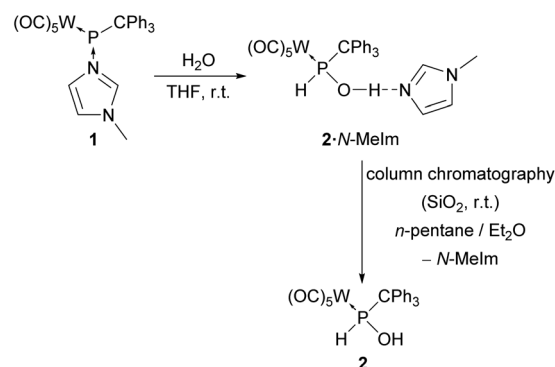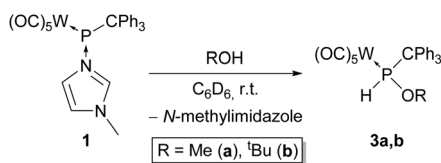

**Scheme 1** Hydrolysis of complex **1**.
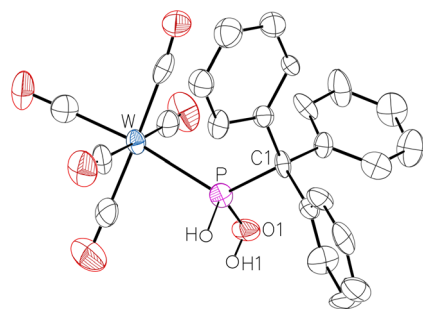
Fig. 2 Molecular structure of **2**. Thermal ellipsoids are set at 50% probability and hydrogen atoms are omitted for clarity except for those bound to phosphorus or oxygen atoms. Selected bond lengths/Å and bond angles/°: W–P 2.527(3), P–O1 1.575(8), P–C1 1.919(10), O1–P–W 113.8(3), O1–P–C1 105.8(4), C1–P–W 124.1(3).

Scheme 2 Synthesis of alkoxy(triphenylmethyl)phosphane complexes **3a,b**.

strongly with the increasing steric demand of the organic substituent of the alcohol. For example, the reaction of **1** with methanol was complete within one day, yielding **3**, while the reaction with *tert*-butanol took 14 days to reach completion.

Previous studies on ligand substitution in model complex adduct **1′** (*tert*-butyl instead of trityl group at phosphorus) revealed that both S$_N$1 (elimination–addition) and S$_N$2 (addition–elimination) mechanisms could take place, depending on the incoming ligand.[32] To unveil the exact mechanism involved in the addition of ROH, quantum chemical (QC) calculations were performed for the model reaction of **1′** with MeOH (see the Computational Details section in the ESI†). These calculations suggest some interesting aspects described below. First, the associative (addition of the incoming ligand as the first step) S$_N$2-type mechanism turns out not to be a simple displacement of the nucleofugic *N*-MeIm ligand at P by the incoming MeOH nucleophile but rather seems to start by P-protonation with concomitant deprotonation of the acidic H^2 at the imidazole ligand affording **4′·MeOH** (Scheme 3). The reprotonation of the imidazole C^2 should then occur *via* the addition of the methoxy unit to a carbonyl ligand at the metal fragment (**5′**), which allows intramolecular MeO group transfer to the P atom with the elimination of the *N*-MeIm ligand, affording the final (model) product **3a′** (Scheme 3). The methoxy group transfer can occur from different conformers (**5′ax/5′eq**) that enable either the energetically favoured (axial) approach to phosphorus, with the nucleofuge occupying an axial position, or the less favoured equatorial position, the latter requiring subsequent pseudorotation at the P centre
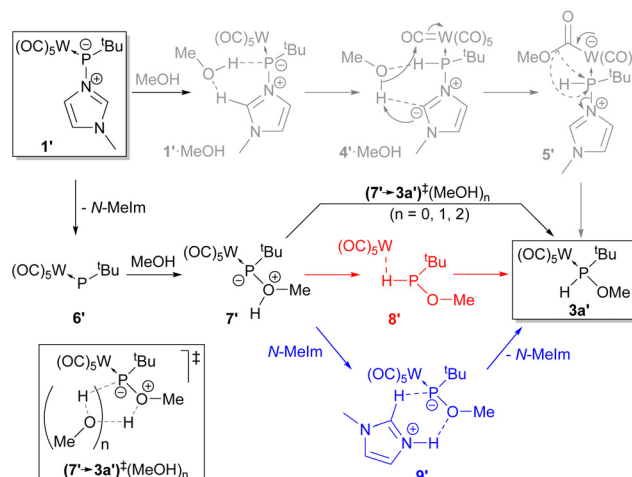
Scheme 3 Proposed mechanism for the addition of MeOH to model complex adduct **1′**.

(Fig. 3). The suggested alternative S$_N$1-like mechanism (Scheme 3) involves the initial rather endergonic dissociation of the *N*-MeIm ligand, affording the terminal phosphinidene intermediate **6′**, followed by thermoneutral addition of MeOH giving rise to the zwitterionic species **7′** (Fig. 3).

The O-to-P proton shift can occur intramolecularly (**7′→3a′**) over a moderately high barrier, or across a lower energy pathway involving simultaneous P-decomplexation (**8′**, the electron rich-metal centre forming a sort of hydrogen bond: $d_{W\cdots H}$ = 1.949 Å, MBO$_{W\cdots H}$ = 0.213; (OC)$_{ax}$–W⋯H angle 164.9°) and followed by small barrier P-complexation.

On the other hand, the O-to-P hydrogen shift can occur intermolecularly by the action of one or two MeOH molecules, (**7′→3a′**)‡(MeOH)$_n$, enabling a proton transfer chain with an increasingly lower energy barrier. The intramolecular transfer can also take place with the lowest computed barrier in two steps involving *N*-MeIm, *via* the imidazolium salt **9′**, constituting the lowest energy pathway for the **7′→3a′** transformation (Scheme 3, Fig. 3).

Therefore, according to these calculations (Fig. 3), the overall minimum energy pathway for the addition of MeOH to **1′** shows some slight preference for the (dissociative) S$_N$1 mechanism (**1′→6′→7′**) with *N*-MeIm-mediated proton migration (**7′→9′→3a′**), although the S$_N$2 pathway is also possible due to the small energy difference. The insertion of water on **1′** is expected to occur by a similar mechanism.

Reactions with strong acids

When strong(er) Brønsted–Lowry acids were added to complex **1** an additional reaction was observed, *i.e.*, formation of *N*-methylimidazolium salts. Therefore, the addition of two equivalents of the acids was essential to reach completion. The reaction of complex **1** with trifluoroacetic acid or hydrogen chloride in dichloromethane resulted in the formation of the *P*-trifluoroacetoxy or *P*-chloride phosphane complexes **10a,b** (Scheme 4). Compound **10b** was already reported and charac-
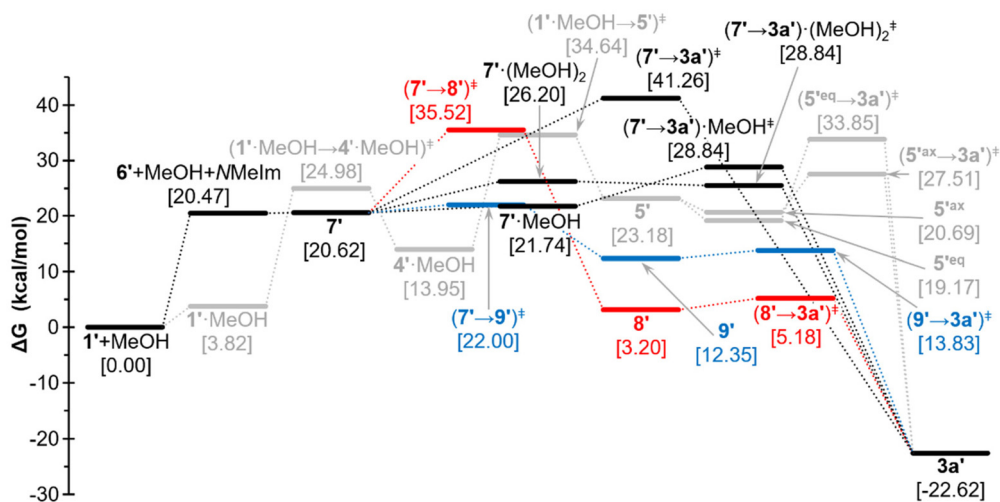
Fig. 3 Computed [CPCM(tol)/PWPB95-D3/def2-QZVPP(ecp)//CPCM(tol)/PBEh-3c] Gibbs energy profile for the addition of methanol to model complex adduct **1'**. Colour code used for S$_N$2- (grey) and S$_N$1-type mechanism with direct or MeOH-assisted H-transfer (black), *N*-MeIm-assisted H-transfer (blue) or involving decomplexation/recomplexation (red).
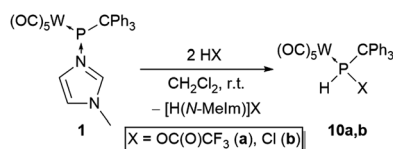

Scheme 4 Synthesis of complexes **10a,b**.

terised in a prior study by us *via* a different route using hydrogen chloride to substitute a P-bound *tert*-butylamino group.[35] The products were extracted with *n*-pentane (**10a**) or diethyl ether (**10b**) from the residue containing *N*-methylimidazolium trifluoroacetate or chloride, respectively, thus obtaining both products in good yields.

The ^{31}P NMR spectrum of **10a** showed a downfield-shifted resonance signal at 112.1 ppm compared to the hydroxyphosphane (phosphinous acid) **2** and alkoxyphosphane (phosphinous ester) complexes **3a,b** whereas **10b** appeared at higher field (71.2 ppm). The large, pure negative inductive effect of the perfluorinated acetoxy group, exerted *via* the P–C σ bond, seems to be the origin of this deshielding effect. In the same vein, the $^1J_{P,H}$ coupling constant of **10a** was significantly larger compared to complexes **2**, **3** and **10b** and, accordingly, also the P–*H* proton (8.42 ppm, $^2J_{W,H} = 7$ Hz).

Single crystals suitable for X-ray diffraction analysis of **10a** were obtained; the results confirmed the proposed molecular structure clearly showing the P–O connectivity (Fig. 4). It should be noted that the new protocol has furnished **10b** with significantly improved yields (>99%) compared to 53% *via* the old route.[35]

Reactions with acids possessing weakly coordinating anions

To avoid the substitution of the P-bound *N*-methylimidazole of complex **1** by the acid counteranions, the reactivity of **1** towards three different super-strong acids with weakly coordi-
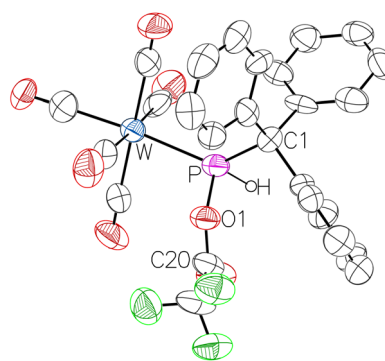
Fig. 4 Molecular structure of **10a**. Thermal ellipsoids are set at 50% probability and hydrogen atoms are omitted for clarity except for the one bound to phosphorus. Selected bond lengths/Å and bond angles/°: W–P 2.452(3), P–O1 1.695(9), P–C1 1.915(12), O1–P–W 106.6(3), O1–P–C1 97.5(5), C1–P–W 130.6(4), C20–O1–P 124.0(9).

nating anions (WCAs)[36] was examined. The reaction of **1** with one equivalent of trifluoromethanesulfonic acid led to the selective formation of the *N*-MeIm-stabilised phosphenium complex **11a** bearing trifluoromethanesulfonate as counteranion (Scheme 5).
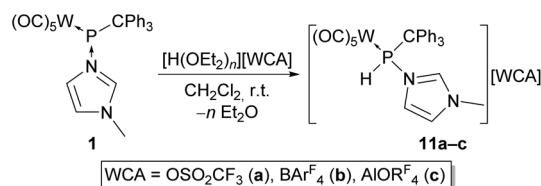
Scheme 5 Synthesis of phosphanylimidazolium complex salts **11a–c** (BAr$^F_4$ = tetrakis{3,5-bis(trifluoromethyl)phenyl}borate, AlOR$^F_4$ = tetrakis(nonafluoro-*tert*-butoxy)aluminate).
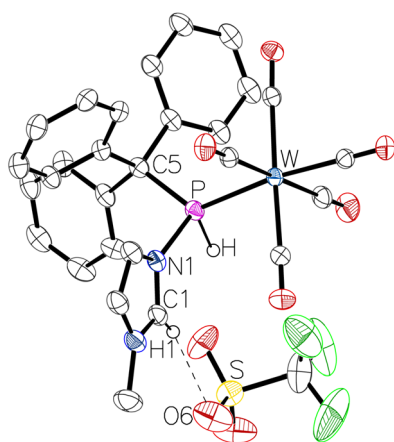
The ^{31}P NMR spectrum of **11a** displayed a resonance at 65.5 ppm ($^{1}J_{P,H}$ = 373 Hz, $^{1}J_{W,P}$ = 278 Hz). The highfield shift compared to complexes **10a,b** suggests the presence of the P-bound donor. Interestingly, we noted that the PH and C^{2}H protons exhibited similar deshielded resonance signals in the ^{1}H NMR spectrum (Table 1). The assumption that the deshielding of the C^{2}H proton stems from unexpected hydrogen bonding with the trifluoromethanesulfonate anion was finally confirmed by X-ray diffraction analysis, revealing an O6–H1 distance of 2.405 Å (Fig. 5; please note that here C1 equals C^{2} in the NMR experiments). Seemingly the P-protonation leads to an enhanced partial positive charge at the phosphorus and the *N*-MeIm unit, thus creating a significant increase in the acidic character of the PH and C^{2}H hydrogen atoms.

When the reaction of complex **1** with Brookhart's acid[37] [H(OEt$_2$)$_2$][BAr$^{F}_4$] was performed (Scheme 5), the resulting complex cation was even more separated from the anion, namely tetrakis[3,5-bis(trifluoromethyl)phenyl]borate. In this case, the phosphorus resonance of **11b** was at 77.7 ppm ($^{1}J_{P,H}$ = 353 Hz, $^{1}J_{W,P}$ = 284 Hz), further downfield-shifted compared to **11a**. The distinct solvent separation became clear from the ^{1}H NMR spectrum as a strong highfield-shifted C^{2}H resonance was detected thus providing strong evidence for the loss of the hydrogen bond of the anion to the C^{2}H proton. The molecular structure of **11b** was confirmed by single-crystal X-ray diffraction analysis (Fig. 6).

To garner further support for the influence of the anion on the cationic part and, hence, the deshielding effects, complex **1** was treated with Krossing's acid [H(OEt$_2$)$_2$][Al{OC(CF$_3$)$_3$}$_4$],[38] yielding the corresponding aluminate salt **11c** (Scheme 5). As anticipated, the tetrakis(nonafluoro-*tert*-butoxy)aluminate ([AlOR$^{F}_4$]$^{-}$) did not cause a significant change in the ^{31}P or ^{1}H NMR parameters of **11c** (77.8 ppm, $^{1}J_{P,H}$ = 354 Hz, $^{1}J_{W,P}$ = 284 Hz) compared to **11b**. To experimentally address the bonding situation within the *N*-methylimidazole donor, gradient-enhanced (ge) 2D NMR ^{1}H,^{15}N heteronuclear multiple bond correlation (HMBC) experiments were conducted.

The difference of the ^{15}N NMR chemical shifts of N^{1} and N^{3} in complexes **11a–c** is small compared to complex **1** (Table 1), suggesting a significant delocalisation of the positive charge within the imidazolium ring of complexes **11a–c** as expected. Interestingly, the ^{15}N NMR chemical shifts of the nitrogen nuclei of **11a** were most similar, supposing a stronger stabilisation of the positive charge in the imidazolium ring due to the coordination of the trifluoromethanesulfonate to the C^{2}H proton. The molecular structure of complex **11c** was also confirmed by single crystal X-ray diffraction analysis (see ESI Fig. S108†), but the data quality does not justify any further discussion of structural parameters.

As phosphanylimidazolium complexes **11a–c** can also be formally described as *N*-methylimidazole-to-phosphenium complex adducts **11^{dat}a–c** (Fig. 7), we became interested in a more in-depth theoretical P–N bonding analysis. Experimentally, the description of **11^{dat}a–c**, implying a weak

Table 1 Selected ^{1}H and ^{15}N NMR data of complexes **1**, **11a–c**, **12** and respective pentacarbonylchromium(0) complexes

Entry	δ(^{1}H)/ppm		δ(^{15}N)/ppm		
	C^{2}–H	P–H	N–CH$_3$	N–P	|Δδ(^{15}N)|/ppm
1[32]	6.41	—	−215.2	−183.9	31.3
11a	9.12	9.41	−205.0	−200.3	4.7
11b	7.26	8.84	−203.1	−194.6	8.5
11c	7.27	8.84	−204.2	−195.7	8.5
12	8.71	—	−202.4	−191.4	11.0
1-Cr[32],*a*	6.45	—	−215.2	−177.7	37.5
11a-Cr^{a}	9.11	8.94	−205.8	−200.3	5.5
11c-Cr^{a}	7.20	8.34	−204.2	−195.7	8.5
12-Cr^{a}	8.66	—	−203.1	−191.4	11.7

^{a} "–Cr" denotes the respective pentacarbonylchromium(0) complexes, obtained similarly, as explained in the ESI.†
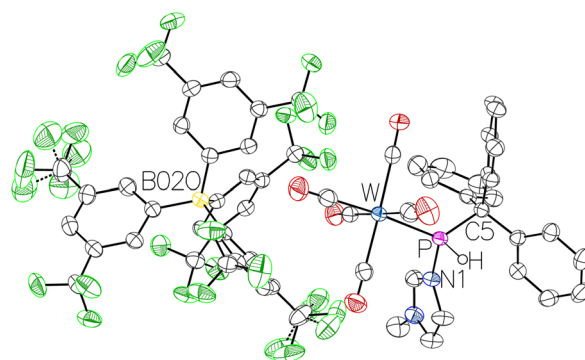

Fig. 5 Molecular structure of **11a**. Thermal ellipsoids are set at 50% probability and hydrogen atoms are omitted for clarity except for those bound to phosphorus or involved in hydrogen bonding. Selected bond lengths/Å and bond angles/°: W–P 2.4815(12), P–C5 1.894(5), P–N1 1.776(4), O6–H1 2.40499(10), N1–P–W 110.94(14), N1–P–C5 103.78(19), C5–P–W 127.57(15).

Fig. 6 Molecular structure of **11b**. Thermal ellipsoids are set at 50% probability and solvent molecules and hydrogen atoms are omitted for clarity except for the one bound to phosphorus. Selected bond lengths/Å and bond angles/°: W–P 2.4611(4), P–N1 1.7773(14), P–C5 1.9239(16), N1–P–W 113.30(5), N1–P–C5 102.46(7), C5–P–W 130.29(5).
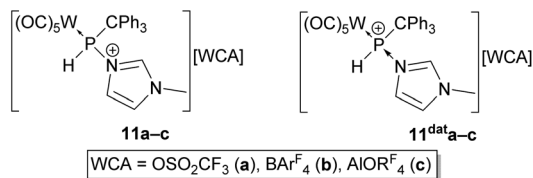
Fig. 7 Canonical structures of complexes **11a–c**, including the formal representation as *N*-methylimidazole-to-phosphenium complex adducts **11$^{\text{dat}}$a–c**.

P–N bond interaction, was supported by the finding that the mass spectrum of complex **11b** showed the *P*–H substituted phosphenium complex (*m/z* 599.0) as the base peak, providing first evidence for the ease of P–N bond cleavage under mass spectrometry conditions.

Two model *P*–H substituted phosphenium complex adducts [^{t}Bu-PH(L)–W(CO)$_5$]$^{+}$ were analysed by quantum chemical calculations. The profile of the Laplacian of the electron density along the central part of the L–P bond path has been shown to have diagnostic character to typify its dative or covalent bonding nature.[32,39] In the case of neutral **3a′** (L: MeO^{-}) two valence–shell charge concentration (VSCC) bands (Fig. 8), corresponding to the two atoms engaged in the bond, appear within the basin of the donor atom (O) delimited by the bond critical point (BCP). Within the framework of the quantum theory of atoms-in-molecules (AIM),[40] a BCP is a point between two atoms where the gradient of the electron density with respect to the spatial coordinates is zero, indicating a minimum in electron density along the bond path. The positive and relatively large value of the Laplacian at the BCP ($\nabla^2\rho$ = 13.43 e Å^{-5}) points to an essentially covalent nature of the P–OMe bond in **3a′**.

Similarly, in case of model cation **11′$^{+}$** (L: *N*-MeIm), the two VSCC bands are located at the basin of the N donor atom (τ_{VSCC} = 0.0423), but the very decreased positive value of the Laplacian of the electron density at the BCP ($\nabla^2\rho$ = 4.21 e Å^{-5})

is indicative of the mostly dative character of the N → P bond, thus paralleling the reported behaviour for phosphinidene complex adduct **1**,[32] and confirming the best description as **11$^{\text{dat}}$a–c** (Fig. 8) for products arising from protonation with super-strong acids having WCAs.

Facile P–H deprotonation

The P-bound proton in complexes **11a–c** is expected to have a highly acidic character due to the proposed significant phosphenium character. This should be very pronounced for complexes **11b,c** since the anions display "innocent" behaviour and no additional interaction with the C^{2}–H proton was detected spectroscopically by NMR. Interestingly, when complex **11c** was dissolved in tetrahydrofuran or tetrahydrofuran-d_8 an immediate colour change from colourless to yellow was observed, and the ^{1}H and ^{31}P NMR spectra showed the reformation of the *N*-methylimidazole-to-phosphinidene complex adduct **1**, thus revealing a surprisingly facile deprotonation at the *P*-centre by the very weak base THF (Scheme 6).

Since no polymerization of the solvent was observed, and a slightly broadened signal at 7.62 ppm with an integral of 1 proton appeared in the ^{1}H NMR spectrum (see ESI Fig. S74†) when dissolved in THF-d_8, we assume that [H(thf-d_8)$_2$][AlOR$^{\text{F}}_4$] was formed, especially as the ^{1}H NMR data are in good accordance with those reported for the respective non-deuterated acid by Krossing when dichloromethane-d_2 was used as solvent.[38]

The gas-phase acidity, in terms of Gibbs free energy ΔG_{acid} (kcal mol^{-1}), was computed as reported elsewhere,[41] uncovering a remarkable value for **11′$^{+}$** (244.4), slightly larger than that of Me$_2$C=OH^{+} (188.9) and Me$_3$PH^{+} (222.8), but significantly lower than that of CF$_3$SO$_3$H (293.6; 299.5[42]), differently substituted imidazoles (299.4–343.9)[43] or CH$_3$COOH (341.5; 341.1[44]).

P-Alkylation of the *N*-MeIm-to-phosphinidene complex adduct

To get access to more inert formal *N*-methylimidazole-to-phosphenium complex adducts, the P-alkylation was examined to avoid unwanted acid–base reactions. Complex **1** reacted with methyl trifluoromethanesulfonate in a clean fashion (Scheme 7), and the ^{31}P NMR resonance signal of the selectively formed *N*-methylimidazole-to-methyl(triphenylmethyl)phosphenium complex adduct **12** was observed at 116.4 ppm ($^{1}J_{\text{W,P}}$ = 274 Hz). Complex **12** was easily isolated *via* crystallization from a diethylether/THF mixture at −40 °C.

The differences in the ^{15}N NMR chemical shifts of the two nitrogen nuclei in complex **12** are more than doubled ($\Delta\delta(^{15}$N)
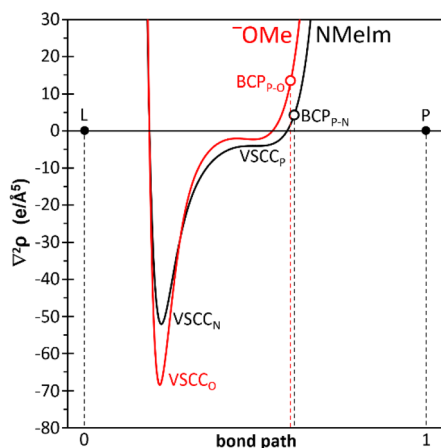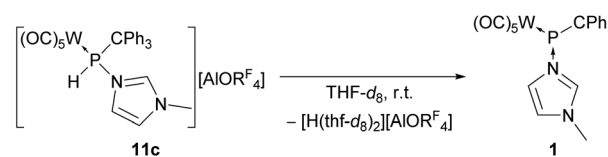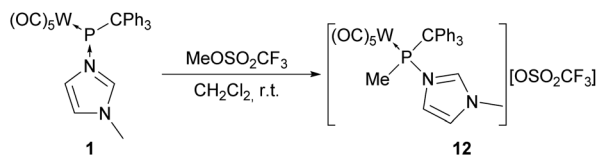

Fig. 8 Computed [B3LYP-D3/def2-TZVPP(ecp)//B3LYP-D3/def2-TZVP (ecp)] variation of the Laplacian of electron density $\nabla^2\rho$ for **3a′** (red) and **11′$^{+}$** (black) along the L–P bond path.

Scheme 6 Deprotonation of the phosphanylimidazolium complex **11c** in THF-d_8 to complex **1** and the proposed formation of [H(thf-d_8)$_2$][AlOR$^{\text{F}}_4$].

Scheme 7 Synthesis of methylphosphanylimidazolium complex **12**.

= 11.0 ppm) compared to those of complexes **11a–c** again indicating weaker P–N interactions resulting in an increased phosphenium character. Nevertheless, the $\Delta\delta(^{15}N)$ value is still relatively small compared to the one of complex **1**, suggesting that the positive charge still is significantly located within the *N*-methylimidazole moiety. These observations are in good accordance with the Laplacian of the electron density $\nabla^2\rho_{P-L}$ (**11′+** (4.21 e Å^{-5}) > **12′+** (3.74 e Å^{-5}) > **1′** (3.15 e Å^{-5})[32]) and with the (natural) charge transfer $q^N(L)$ from the *N*-MeIm ligand (**11′+** (0.409 e) > **12′+** (0.386 e) > **1′** (0.320 e)). Noteworthy, this trend is not in line with the differences in natural charges at the *N*-MeIm ligand $q^N(N3)–q^N(N1)$ (**1′** (0.207 e) ≪ **11′+** (0.280 e) < **12′+** (0.293 e)).

Unexpectedly, the ^1H and $^{13}C\{^1H\}$ NMR spectra of complex **12** revealed a more complicated pattern of resonance signals for the triphenylmethyl group in which the nuclei of every phenyl group were magnetically different, thus indicating a hindered rotation at the P–C bond. Particularly, the *ortho*-C*H* protons differed significantly for each phenyl group with broad resonance signals at 7.64, 7.30 and 6.61 ppm. This indicates the increased steric hindrance at phosphorus due to the P-bound methyl group. Again a weak P–N interaction was indicated by the mass spectrum of **12** as the phosphenium complex (*m/z* 613.0) and the free phosphenium cation [P(CPh$_3$)Me]$^+$ (*m/z* 289.1) were detected.

The greater stability of the *P*-Me derivative **12** enabled to grow single crystals suitable for X-ray diffraction analysis (Fig. 9).
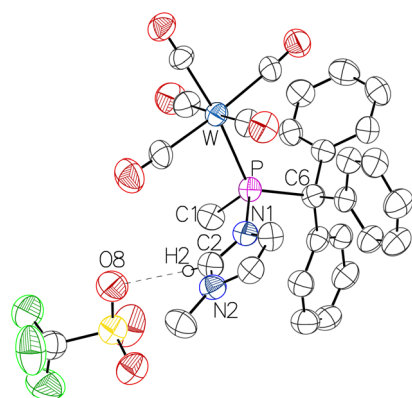
As expected, the molecular structure of **12** revealed the hydrogen bond interaction between the anion and the C^2-bound hydrogen (O8–H2 distance: 2.322 Å). The P1–N1 distance of 1.801(6) Å is slightly shorter than the one in complex **1** (1.813 Å)[32] indicating a slightly stronger P–N bond and, hence, a less dative (more covalent) character. However, the N1–C2 and N2–C2 bond lengths are similar, indicating a considerably stronger covalency (higher $\nabla^2\rho_{P-N}$) of the P–N bond together with a pronounced contribution of a delocalised positive charge within the imidazole ring compared to complex **1**.

Conclusions

We have demonstrated that the *N*-methylimidazole-to-phosphinidene complex adduct **1** undergoes 1,1-addition reactions with weak Brønsted–Lowry acids, such as water and alcohols, by displacing the donor entity. When complex **1** was treated with stronger acids HX, such as trifluoroacetic acid and hydrogen chloride, two equivalents of the acid were needed to complete the 1,1-addition reaction, as the released *N*-methylimidazole formed rapidly the respective *N*-methylimidazolium salts. To avoid substitution and achieve exclusively the P-protonation of complex **1**, reactions with super-strong acids were performed, having weakly coordinating anions (WCA), *i.e.*, trifluoromethanesulfonic acid, Brookhart's acid [H(OEt$_2$)$_2$][BAr$_4^F$] and Krossing's acid [H(OEt$_2$)$_2$][AlOR$_4^F$]. In all cases, P-protonation and salt formation were achieved, but the anion–cation interaction was different. Remarkably, an increased acidity of the P-bound proton was disclosed in the case of the aluminate salt which was analysed by theory. In total, a novel access to donor-stabilised phosphenium complexes bearing a P–H bond has been developed, including an in-depth analysis of the P–N bonding.

Data availability

Synthetic details and analytical data, including depictions of all spectra and detailed accounts of the methods applied are documented in the ESI.†

Author contributions

DB planned and carried out the experiments and collected and evaluated analytical data. GS measured and evaluated the crystallographic data. AEF carried out the theoretical study and the discussion. RS provided the concept and the supervision of the investigation. DB, AEF and RS wrote the manuscript. The ESI† was prepared by DB, AEF and RS.

Conflicts of interest

There are no conflicts to declare.

Fig. 9 Molecular structure of **12**. Thermal ellipsoids are set at 50% probability and solvent molecules and hydrogen atoms are omitted for clarity except for the one involved in hydrogen bonding. Selected bond lengths/Å and bond angles/°: W–P 2.4996(19), P–N1 1.801(6), P–C1 1.837(7), P–C6 1.947(7), O8–H2 2.32189(10), N1–C2 1.335(9), N2–C2 1.321(9), N1–P–W 109.4(2), N1–P–C1 97.1(3), N1–P–C6 104.6(3), C1–P–W 111.5(3), C1–P–C6 106.3(3), C6–P–W 124.3(2).

References

1 (a) R. Allmann, *Chem. Ber.*, 1966, **99**, 1332; (b) R. Allmann, *Angew. Chem., Int. Ed. Engl.*, 1965, **4**, 150; (c) K. Dimroth and P. Hoffmann, *Chem. Ber.*, 1966, **99**, 1325; (d) K. Dimroth and P. Hoffmann, *Angew. Chem., Int. Ed. Engl.*, 1964, **3**, 384.

2 M. G. Thomas, C. W. Schultz and R. W. Parry, *Inorg. Chem.*, 1977, **16**, 994.

3 S. Fleming, M. K. Lupton and K. Jekot, *Inorg. Chem.*, 1972, **11**, 2534.

4 B. E. Maryanoff and R. O. Hutchins, *J. Org. Chem.*, 1972, **37**, 3475.

5 (a) P. Friedrich, G. Huttner, J. Luber and A. Schmidpeter, *Chem. Ber.*, 1978, **111**, 1558; (b) J. Luber and A. Schmidpeter, *Angew. Chem., Int. Ed. Engl.*, 1976, **15**, 111.

6 I. A. Litvinov, V. A. Naumov, T. V. Griaznova, A. N. Pudovik and A. M. Kibardin, *Dokl. Akad. Nauk SSSR*, 1990, **312**, 3159.

7 M. K. Denk, S. Gupta and A. J. Lough, *Eur. J. Inorg. Chem.*, 1999, **1999**, 41.

8 D. Gudat, A. Haghverdi, H. Hupfer and M. Nieger, *Chem. – Eur. J.*, 2000, **6**, 3414.

9 (a) S. Pohl, *Chem. Ber.*, 1979, **112**, 3159; (b) E. Niecke and R. Kröher, *Angew. Chem., Int. Ed. Engl.*, 1976, **15**, 692.

10 M. Olaru, S. Mebs and J. Beckmann, *Angew. Chem., Int. Ed.*, 2021, **60**, 19133.

11 (a) M. Yoshifuji, *Sci. Synth.*, 2009, **42**, 63; (b) A. H. Cowley and R. A. Kemp, *Chem. Rev.*, 1985, **85**, 367.

12 D. Gudat, E. Niecke, B. Krebs and M. Dartmann, *Chimia*, 1985, **39**, 277.

13 D. Gudat, M. Nieger and E. Niecke, *J. Chem. Soc., Dalton Trans.*, 1989, 693.

14 S. Loss, C. Widauer and H. Grützmacher, *Angew. Chem., Int. Ed.*, 1999, **38**, 3329.

15 (a) S. S. Chitnis and N. Burford, *Dalton Trans.*, 2015, **44**, 17; (b) N. Burford, P. Losier, A. D. Phillips, P. J. Ragogna and T. S. Cameron, *Inorg. Chem.*, 2003, **42**, 1087; (c) N. Burford, P. J. Ragogna, R. McDonald and M. J. Ferguson, *J. Am. Chem. Soc.*, 2003, **125**, 14404; (d) N. Burford, P. J. Ragogna, K. N. Robertson, T. S. Cameron, N. J. Hardman and P. P. Power, *J. Am. Chem. Soc.*, 2002, **124**, 382; (e) N. Burford, T. S. Cameron, P. J. Ragogna, E. Ocando-Mavarez, M. Gee, R. McDonald and R. E. Wasylishen, *J. Am. Chem. Soc.*, 2001, **123**, 7947; (f) N. Burford, T. Stanley Cameron, K. N. Robertson, A. D. Phillips and H. A. Jenkins, *Chem. Commun.*, 2000, 2087; (g) N. Burford, T. S. Cameron, D. J. LeBlanc, P. Losier, S. Sereda and G. Wu, *Organometallics*, 1997, **16**, 4712; (h) N. Burford, P. Losier, P. K. Bakshi and T. S. Cameron, *Chem. Commun.*, 1996, 307; (i) N. Burford, T. S. Cameron, J. A. C. Clyburne, K. Eichele, K. N. Robertson, S. Sereda, R. E. Wasylishen and W. A. Whitla, *Inorg. Chem.*, 1996, **35**, 5460; (j) N. Burford, J. A. C. Clyburne, P. K. Bakshi and T. S. Cameron, *Organometallics*, 1995, **14**, 1578; (k) N. Burford, J. A. C. Clyburne, P. Losier, T. M. Parks, T. S. Cameron and J. F. Richardson, *Phosphorus, Sulfur Silicon Relat. Elem.*, 1994, **93**, 301; (l) N. Burford, P. Losier, S. V. Sereda, T. S. Cameron and G. Wu, *J. Am. Chem. Soc.*, 1994, **116**, 6474.

16 L. Rosenberg, *Coord. Chem. Rev.*, 2012, **256**, 606.

17 D. Gudat, A. Haghverdi and M. Nieger, *J. Organomet. Chem.*, 2001, **617–618**, 383.

18 A. E. R. Watson, M. J. Grant, P. D. Boyle, P. J. Ragogna and J. B. Gilroy, *Inorg. Chem.*, 2022, **61**, 18719.

19 (a) P. Ai, C. Gourlaouen, A. A. Danopoulos and P. Braunstein, *Inorg. Chem.*, 2016, **55**, 1219; (b) A. Kozma, T. Deden, J. Carreras, C. Wille, J. Petušková, J. Rust and M. Alcarazo, *Chem. – Eur. J.*, 2014, **20**, 2208; (c) S. Saleh, E. Fayad, M. Azouri, J.-C. Hierso, J. Andrieu and M. Picquet, *Adv. Synth. Catal.*, 2009, **351**, 1621; (d) J. Andrieu, M. Azouri and P. Richard, *Inorg. Chem. Commun.*, 2008, **11**, 1401; (e) Y. Yamaguchi, H. Nakazawa, M. Kishishita and K. Miyoshi, *Organometallics*, 1996, **15**, 4383; (f) H. Nakazawa, Y. Yamaguchi, T. Mizuta, S. Ichimura and K. Miyoshi, *Organometallics*, 1995, **14**, 4635; (g) R. W. Parry and J. M. Higashi, *J. Fluorine Chem.*, 1995, **71**, 221.

20 S. M. Rocklage, R. R. Schrock, M. R. Churchill and H. J. Wasserman, *Organometallics*, 1982, **1**, 1332.

21 (a) R. Schmitt, PhD thesis, University of Würzburg, 2005; (b) E. Urnezius, S. J. Klippenstein and J. D. Protasiewicz, *Inorg. Chim. Acta*, 2000, **297**, 181; (c) W. Malisch, U.-A. Hirth, K. Grün and M. Schmeußer, *J. Organomet. Chem.*, 1999, **572**, 207; (d) U. Segerer and E. Hey-Hawkins, *Polyhedron*, 1997, **16**, 2537; (e) W. Malisch, U.-A. Hirth, K. Grün, M. Schmeusser, O. Fey and U. Weis, *Angew. Chem., Int. Ed. Engl.*, 1995, **34**, 2500; (f) N. C. Zanetti, R. R. Schrock and W. M. Davis, *Angew. Chem., Int. Ed. Engl.*, 1995, **34**, 2044; (g) E. Hey-Hawkins and K. Fromm, *Polyhedron*, 1995, **14**, 2825; (h) M. C. Fermin, J. Ho and D. W. Stephan, *J. Am. Chem. Soc.*, 1994, **116**, 6033; (i) E. Hey-Hawkins and S. Kurz, *J. Organomet. Chem.*, 1994, **479**, 125; (j) J. Ho, R. Rousseau and D. W. Stephan, *Organometallics*, 1994, **13**, 1918; (k) W. Malisch, U.-A. Hirth, T. A. Bright, H. Käb, T. S. Ertel, S. Hückmann and H. Bertagnolli, *Angew. Chem., Int. Ed. Engl.*, 1992, **31**, 1525.

22 R. Menye-Biyogo, F. Delpech, A. Castel, V. Pimienta, H. Gornitzka and P. Rivière, *Organometallics*, 2007, **26**, 5091.

23 M. P. Duffy, L. Y. Ting, L. Nicholls, Y. Li, R. Ganguly and F. Mathey, *Organometallics*, 2012, **31**, 2936.

24 L. L. Liu, D. A. Ruiz, F. Dahcheh and G. Bertrand, *Chem. Commun.*, 2015, **51**, 12732.

25 (*a*) K. Lammertsma, *Top. Curr. Chem.*, 2003, **229**, 95; (*b*) F. Mathey, N. H. T. Huy and A. Marinetti, *Helv. Chim. Acta*, 2001, **84**, 2938.

26 A. Marinetti, F. Mathey, J. Fischer and A. Mitschler, *J. Am. Chem. Soc.*, 1982, **104**, 4484.

27 F. Mercier, B. Deschamps and F. Mathey, *J. Am. Chem. Soc.*, 1989, **111**, 9098.

28 (*a*) R. Streubel, *Top. Curr. Chem.*, 2002, **223**, 91; (*b*) R. Streubel, *Coord. Chem. Rev.*, 2002, **227**, 175; (*c*) R. Streubel, A. Kusenberg, J. Jeske and P. G. Jones, *Angew. Chem., Int. Ed. Engl.*, 1995, **33**, 2427; (*d*) R. Streubel, J. Jeske, P. G. Jones and R. Herbst-Irmer, *Angew. Chem., Int. Ed. Engl.*, 1994, **33**, 80.

29 M. L. G. Borst, R. E. Bulo, C. W. Winkel, D. J. Gibney, A. W. Ehlers, M. Schakel, M. Lutz, A. L. Spek and K. Lammertsma, *J. Am. Chem. Soc.*, 2005, **127**, 5800.

30 (*a*) A. Schmer, P. Junker, A. Espinosa Ferao and R. Streubel, *Acc. Chem. Res.*, 2021, **54**, 1754; (*b*) A. Ozbolat, G. von Frantzius, J. M. Pérez, M. Nieger and R. Streubel, *Angew. Chem., Int. Ed.*, 2007, **46**, 9327.

31 I. Kalinina and F. Mathey, *Organometallics*, 2006, **25**, 5031.

32 D. Biskup, G. Schnakenburg, R. T. Boeré, A. Espinosa Ferao and R. K. Streubel, *Nat. Commun.*, 2023, **14**, 6456.

33 D. Biskup, G. Schnakenburg, R. T. Boeré, A. Espinosa Ferao and R. Streubel, *Dalton Trans.*, 2023, **52**, 13781.

34 R. Streubel, A. W. Kyri, L. Duan and G. Schnakenburg, *Dalton Trans.*, 2014, **43**, 2088.

35 R. Streubel, A. Schmer, A. W. Kyri and G. Schnakenburg, *Organometallics*, 2017, **36**, 1488.

36 I. M. Riddlestone, A. Kraft, J. Schaefer and I. Krossing, *Angew. Chem., Int. Ed.*, 2018, **57**, 13982.

37 M. Brookhart, B. Grant and A. F. Volpe, *Organometallics*, 1992, **11**, 3920.

38 I. Krossing and A. Reisinger, *Eur. J. Inorg. Chem.*, 2005, **2005**, 1979.

39 (*a*) A. Espinosa Ferao, A. García Alcaraz, S. Zaragoza Noguera and R. Streubel, *Inorg. Chem.*, 2020, **59**, 12829; (*b*) V. Nesterov, R. Baierl, F. Hanusch, A. E. Ferao and S. Inoue, *J. Am. Chem. Soc.*, 2019, **141**, 14576; (*c*) M. W. Stanford, J. I. Schweizer, M. Menche, G. S. Nichol, M. C. Holthausen and M. J. Cowley, *Angew. Chem., Int. Ed.*, 2019, **58**, 1329.

40 (*a*) R. F. W. Bader, *Atoms in molecules. A quantum theory*, Oxford University Press, Oxford, 1990; (*b*) R. F. W. Bader, *Chem. Rev.*, 1991, **91**, 893; (*c*) C. F. Matta and R. J. Boyd, in *The quantum theory of atoms in molecules*, ed. C. F. Matta and R. J. Boyd, Wiley-VCH, New York, 2007, pp. 1–34.

41 (*a*) I. A. Topol, G. J. Tawa, R. A. Caldwell, M. A. Eissenstat and S. K. Burt, *J. Phys. Chem. A*, 2000, **104**, 9619; (*b*) J. L. Chen, L. Noodleman, D. A. Case and D. Bashford, *J. Phys. Chem.*, 1994, **98**, 11059.

42 I. A. Koppel, R. W. Taft, F. Anvia, S.-Z. Zhu, L.-Q. Hu, K.-S. Sung, D. D. DesMarteau, L. M. Yagupolskii and Y. L. Yagupolskii, *J. Am. Chem. Soc.*, 1994, **116**, 3047.

43 N. Wang and J. K. Lee, *J. Org. Chem.*, 2019, **84**, 14593.

44 S. G. Lias, J. E. Bartmess, J. F. Liebman, J. L. Holmes, R. D. Levin and W. G. Mallard, *J. Phys. Chem. Ref. Data*, 1988, **17**(Suppl. 1).